CHAPTER 5

Transition Zone Width and Implications for Modelling Surfzone Hydrodynamics

Robert B. Nairn[1] , J.A. (Dano) Roelvink[2] and Howard N. Southgate[3]

INTRODUCTION

The surfzone associated with a wave breaking on a plane slope may be subdivided into three regions: the transition zone, the inner zone and the swash zone. The transition zone is the region just shoreward of the point of wave breaking and is characterised by rapid wave decay and also by constant wave setdown (and thus constant radiation stress). In this paper, an empirical expression for the width of this zone is developed from monochromatic wave data. Two techniques are proposed for the consideration of this phenomenon in the numerical modelling of surfzone hydrodynamics for random waves. The implications of a zone of nearly constant radiation stress inside the breakpoint are examined with respect to wave-induced current generation - both cross-shore and longshore - and sediment transport prediction. Comparisons are made to both field and laboratory data from plane and undulating profiles.

BACKGROUND

The existence of a zone of transition between the unbroken wave shape and the turbulent bore form of the broken wave was first reported by Svendsen et al (1978) based on visual observations of wave breaking. Svendsen (1984) proposed a definition of the transition zone as the region of nearly horizontal or very weakly sloping water level inside the breakpoint before the beginning of a steep gradient in the water level due to wave setup.

Both Svendsen (1984) and subsequently Basco and Yamashita (1986), were concerned with the influence of the transition zone on the description of wave height decay and mean water level variation in the surfzone through the solution of the energy and momentum balance equations. The transition zone features rapid wave decay without an associated increase in energy dissipation. Svendsen (1984) suggested that the large amount of potential energy lost in this region is converted to forward

---

[1]Department of Civil Engineering, Imperial College of Science, Technology and Medicine. London, England. SW7 2BU.
[2]Delft Hydraulics. P.O. Box 152, 8300 Emmeloord, The Netherlands.
[3]Hydraulics Research Limited. Wallingford, Oxon., England. OX10 8BA.

momentum flux, specifically in the surface roller. Basco and Yamashita (1986) viewed the process in the transition zone as a transformation from oscillatory wave motion to highly rotational (turbulent) motion. Thus, the region is essentially a development zone where the just broken wave is transformed into a turbulent bore. Basco (1985) notes that both plunging and spilling breakers feature this same development process, albeit at much different scales. Two approaches for considering the role of the transition zone processes in the prediction of wave height decay are presented in the above-noted papers.

A zone of nearly constant mean water level, through consideration of the momentum balance equation, implies that the radiation stress is also constant. Consequently, the generation of wave-induced cross-shore and longshore currents by the reduction in radiation stress due to energy dissipation does not commence until the inner limit of the transition zone is reached. In a comparison of numerical model estimates to laboratory measurements of the distribution of longshore currents across a profile for plunging waves, Visser (1984) found that it was critically important to delay the initiation of the influence of energy dissipation on the generation of longshore currents until the plunge point. As noted by Basco and Yamashita (1986), the distance from the breakpoint to the plunge point is a significant fraction of the transition zone width. A similar influence of the transition zone has been observed in the prediction of wave-induced return flow in the surfzone (or undertow) by Roelvink and Stive (1989), Nairn (1990a) and Okayasu et al (1990).

TRANSITION ZONE WIDTH

Basco and Yamashita (1986) proposed that the width of the transition zone would vary with the surf similarity parameter; the zone would be wider for spilling breakers than for plunging breakers. Whilst this may be so in an absolute sense, considering that the plunging breaker must undergo a much greater change in wave shape, it is more likely that the dimensionless width of the transition zone (normalised by the depth at breaking) will be larger for plunging breakers. An empirical expression can be developed for the dimensionless transition zone width using dimensional analysis techniques. The ratio of the depth at the inner limit of the transition zone, d_t, to the depth at breaking, d_b, is found to be a function of two parameters as follows,

$$\frac{d_t}{d_b} = f\left\{\frac{m_b}{(H_b/L_o)^{0.5}}\ ,\ \frac{d_b}{L_b}\right\} \tag{1}$$

The first variable is the surf similarity parameter, where m_b is the bottom slope in the vicinity of the breakpoint, H_b is the wave height at breaking and L_o is the deepwater wavelength; the second variable is the ratio of the depth at breaking to the wavelength at breaking and provides an indication of the scale of the wave with respect to the width of the surfzone. A data set on the width of the transition zone was gathered from laboratory experiments with monochromatic waves - the width was defined as the distance from the breakpoint to the abrupt change in slope of the mean water level (an example of one of these laboratory experiments is given in Figure 1). By combining the two variables of Equation 1 into a single parameter and performing a regression analysis on the data set, the following relationship was derived,

$$d_t/d_b = 0.47\ \xi_{bb}^{-0.275}\ ,\ for\ \ \xi_{bb} \geq 0.05$$

$$d_t/d_b \sim 1\ ,\ for\ \ \xi_{bb} \leq 0.05$$

$$\xi_{bb} = m_b/(H_b/L_b)^{0.5} \qquad (2)$$

Note that the dimensionless transition zone depth is given as a function of the surf similarity parameter evaluated entirely with breakpoint values. This differs from the conventional surf similarity parameter in that the local wavelength at breaking is used in the definition of wave steepness instead of the deepwater value (thus accounting for the second variable in Equation 1). A comparison of this relationship to the data set is given in Figure 2, the correlation coefficient for the regression analysis was 0.85. As anticipated, the dimensionless width (which varies from 5 to 50 % of a plane sloping surfzone) increases with the surf similarity parameter and consequently is greater for plunging breakers than for spilling breakers. In a random wave climate, the transition zone width will vary according to the surf similarity parameter of each individual wave at breaking.

MODELLING THE INFLUENCE ON WAVE-INDUCED CURRENTS

1) Empirical Approach

A numerical model has been developed for the prediction of cross-shore and alongshore sediment transport on a beach profile. The principal components of the model include: 1) wave transformation based on the technique of Battjes and Janssen (1978) for random waves; 2) a description of the mean cross-shore flows under random waves using an adaptation of the method presented by DeVriend and Stive (1987); 3) prediction of the longshore current variation across the profile employing the technique of Southgate (1989); 4) calculation of the central velocity moments based on the non-linear Vocoidal theory (after Swart, 1978) for time-varying orbital velocities; and 5) prediction of the cross-shore and alongshore sediment transport rates across the profile using a modified version of the Energetics approach which was originally developed for coastal applications by Bailard (1981) and Bowen (1980). The influence of the transition zone primarily affects the calculation of the mean wave-induced cross-shore and longshore currents of steps 2 and 3 above. Of course, this influence will also be transmitted to the calculation of sediment transport rates based on the modified currents.

The Battjes and Janssen (1978) description of random wave transformation at each point across a profile consists of two parameters, the root mean square wave height, H_{rms}, and the fraction of broken waves, Q_b. In this time-averaged approach to modelling random waves, the fraction of broken waves represents the proportion of time that waves are breaking at a given point on the profile over a model time step. Both the techniques of DeVriend and Stive (1987) and Southgate (1989) for wave-induced cross-shore and longshore currents respectively are based on a similar approach to random waves. The principal driving force for currents under breaking waves is represented by the reduction in radiation stress, which in turn may be related to the dissipation of wave energy. Therefore, in a time-averaged sense, a driving force for the currents between any two points on a profile is derived from the local decay in the rms wave height multiplied by the fraction of broken waves. However, the stipulation of the transition zone influence suggests that the incremental increase in the driving force due to the local initiation of wave breaking - represented by the increase in the fraction of broken waves between the two points - should be delayed by a distance equivalent to the transition zone width. Therefore, at each point across the profile a revised value of the fraction of broken waves is determined by delaying the incremental increase in Q_b for a distance equivalent to the local transition zone width (i.e. using the local wave height, wavelength and beach slope in Equation 2). The revised Q_b is treated as a new variable and is used in the calculation of energy dissipation for the driving force of radiation stress related quantities such as mean currents and wave setup. A comparison of the revised Q_b to the actual Q_b is presented in Figure 3 which shows the details of the prediction of wave transformation across a profile corresponding to Case 5 of the DUCK85 sediment transport field experiments (this experiment is discussed in more detail later). The revised Q_b distribution is shifted onshore approximately 10 m for this example.

2) Analytical Approach

The mean wave energy balance equation:

$$\frac{\partial}{\partial x} EC_g = S \qquad (3)$$

where E is the mean wave energy, C_g the group velocity and S a (negative) source term, has been used successfully to describe the decay of organised wave energy by means of a bore model. Battjes and Janssen (1978) extended the formulation to the case of random waves by assuming a parametric shape for the wave height distribution. If it is assumed that the organised wave energy is instantly converted to isotropic turbulence energy, the horizontal cross-shore momentum balance reads:

$$\frac{\partial}{\partial x} \tilde{S}_{xx} + \rho g h \frac{\partial \eta}{\partial x} + \tau_b = 0 \qquad (4)$$

where S_{xx} with a tilde is the radiation stress related to the organised wave motion , ρ is the density of water, g the acceleration of gravity, h the water depth, η the mean water level and τ_b the bottom shear stress. Since the term τ_b is generally small, the setup should respond directly to the radiation stress gradients. As has been noted previously, this is not the case; this means that an additional term should exist in the momentum balance equation.

Svendsen (1984) suggested that part of the organised wave energy is first converted into forward momentum flux in the roller, and accounted for this roller influence both in the energy balance, by means of a term:

$$E_r = \rho A C^2/2L = \rho AC/2T \qquad (5)$$

where A is the roller area, C is the phase velocity and T the wave period, and in the momentum balance by means of a term:

$$S_{xx,\,roller} = \rho AC^2/L = \rho AC/T = 2E_r \tag{6}$$

The equations for the energy balance and the momentum balance can then be written respectively as:

$$\frac{\partial}{\partial x} EC_g + \frac{\partial}{\partial x} E_r C = -D \tag{7}$$

where D is the dissipation per unit area, and:

$$\frac{\partial}{\partial x} \tilde{S}_{xx} + \frac{\partial}{\partial x} 2E_r + \rho g h \frac{\partial \eta}{\partial x} + \tau_b = 0 \tag{8}$$

Svendsen (1984) then relates the roller area directly to the local wave height H by using the empirical finding:

$$A = 0.9\ H^2 \tag{9}$$

When this formulation is used, the absolute magnitude of the setup changes, but the spatial distribution of the setup remains directly linked to the wave energy decay, and no transition zone lag effect is found.

On the other hand, Roelvink and Stive (1989) suggested that the organised wave energy is first converted to turbulent kinetic energy which is not dissipated immediately. They proposed to use a k-equation in which the production of turbulent kinetic energy is equal to the decay of organised wave energy:

$$\frac{\partial}{\partial x} EC_g + \frac{\partial}{\partial x} \beta_f khC = -\rho\, \beta_d\, k^{3/2} \tag{10}$$

where k is the depth- and time-mean turbulence intensity and β_f and β_d are coefficients of order one. The second term in this equation represents a storage term, whereas the term on the right is the actual dissipation. Due to the storage term, which is positive in the area of initial decay of wave energy, the dissipation lags behind the production of turbulence energy. The influence of the turbulence on the momentum balance was estimated as:

$$S_{xx,\,turbulence} = \overline{\int_{-d}^{\eta} (\rho u'^2 - \rho w'^2)\, dz} \sim \beta_s\, \rho k h \tag{11}$$

so the momentum balance in this case reads:

$$\frac{\partial}{\partial x} \tilde{S}_{xx} + \frac{\partial}{\partial x} \beta_s\, \rho k h + \rho g h \frac{\partial \eta}{\partial x} + \tau_b = 0 \tag{12}$$

The value of β_s depends on the ratio between the turbulence intensities in the x, y and z-directions; based on the analogy of a wake, a value of 0.22 was suggested. The result was that hardly any influence on the setup distribution was found, although there was a significant lag between the production and dissipation of turbulence energy. This leads to the conclusion that either the turbulence which is generated is much more anistropic than assumed, or that the wave motion is converted into a different form of motion.

A synthesis of these two approaches can be developed using Svendsen's concept of a roller as a 'block' of water moving at the phase velocity, dropping the empirical Equation 9, and assuming the sink term S of the organised wave energy to be a known function of the local wave parameters, as for instance in the Battjes and Janssen model. The roller energy, E_r, in this case becomes the unknown parameter; if the dissipation can be related to this parameter, E_r can be solved from Equation 7. In this way the roller will serve as a storage of kinetic energy, leading to a lag effect similar to that modelled by Equation 10.

The dissipation in this case can be modelled according to Deigaard and Fredsoe (1989) as the work performed by the shear stress, τ_r, between the roller and the organised wave motion:

$$D = \overline{\tau_r}\, C \qquad (13)$$

The shear stress can be deduced by considering the vertical force balance equation on the roller, which leads to:

$$\overline{\tau_r} = \beta\, \rho g A/L \qquad (14)$$

where β is the mean slope under the roller. Combining Equations 13 and 14,

$$D = \beta\, \rho g A/T = 2\beta\, g E_r/h \qquad (15)$$

so Equation 7 can be written as:

$$\frac{\partial}{\partial x} E C_g + \frac{\partial}{\partial x} E_r C = -2\, \beta\, g E_r/C \qquad (16)$$

This equation is quite similar to Equation 10; if it is assumed that $E_r = \rho\, kh$, $C = \sqrt{gh}$ and the order of magnitude estimate $k \sim 1/2\, \beta_1\, C^2$ is taken, the result is:

$$\frac{\partial}{\partial x} E C_g + \frac{\partial}{\partial x} \rho k h C = -\left(2\sqrt{2}\ \beta/\sqrt{\beta_1}\right) \rho\, k^{3/2} \qquad (17)$$

The above expression, with $\beta \sim \beta_1 \sim 0.10$, leads to Equation 10 with $\beta_d \sim 1$.

Comparison of Equations 6 and 11 now shows that the roller contribution to the radiation stress is 0.22 E_r in the turbulence model, against 2 E_r according to the Svendsen concept. In view of the fact that for the first estimate no significant transition zone lag effect in the setup was found, the second estimate seems more realistic. In order to check this, two tests documented in Battjes and Janssen (1978) were hindcast with respect to wave energy decay and setup, specifically, Test HJ2, with a plane beach, and HJ12, with a schematised bar-trough profile. A Battjes type model was used to predict the sink term S; the roller energy E_r was solved both from Equation 10 and from

Equation 16 and the setup was computed from Equation 8. A value for the roller slope of 0.10 was applied in Equation 14. In Figures 4 and 5, the results are presented for the wave energy, represented by $H_{rms} = \sqrt{(8E/\rho g)}$, and for the setup, without the transition zone lag effect and with the lag effect according to both formulations. There is a considerable improvement in the setup prediction in the area of incipient breaking; also, Equations 10 and 16 produce very similar results. With respect to wave-driven currents it is likely that the dissipation rate should be the term D in Equation 7, rather than the sink term S in Equation 1, however formal proof of this has not yet been derived and should be the subject of further study.

The analytical approach described above can be applied to predict the general behaviour of the transition zone width as a function of beach slope and wave steepness. The model was tested for a plane beach with slopes in the range of 0.005 to 0.05 and incident wave steepnesses - defined as H_{rms}/L_o - in the range 0.01 to 0.04. The transition zone width was defined as the distance between the peak of the sink term S and the peak of the dissipation term D, as the peak in S defines the location of maximum gradient in H_{rms}, and the peak in D a location of rapid water level increase. Though this definition differs slightly from that used for the empirical approach, the general behaviour can be expected to be quite similar. The analytical approach may also be applied to either monochromatic or random waves.

The dimensionless transition zone width (i.e. the ratio of the depths at the dissipation peak and the sink term peak) is plotted against the deepwater surf similarity parameter, ξ_o, the similarity parameter at breakpoint values, ξ_{bb}, and against the bottom slope in Figures 6a, b and c respectively. The empirical approach is also plotted in Figure 6b and reasonable agreement with the analytical approach is apparent. Figure 6c demonstrates that the analytical approach is almost entirely dependent on beach slope (there is very little dependence on wave steepness). In contrast, the empirical approach does have a significant dependency on wave steepness based on the monochromatic wave data. The existence of a steepness influence in random waves is indirectly shown in the next section; however, a direct proof of this should be the topic of further study.

COMPARISON TO DATA ON WAVE CURRENT PREDICTION

In this section, examples of the influence of the transition zone width on the prediction of undertow and longshore currents under random waves using the empirical approach are presented. However, the first example relates to the measurement of mean cross-shore flows generated by monochromatic waves. The vertical distributions of mean flow for five locations across a laboratory profile (Case 5 of Nadoaka and Kondoh, 1982) are shown in Figure 7 along with the predicted extent of the transition zone width. Clearly, the measured distribution located between 2 and 3 m on the baseline - which is shoreward of the breakpoint and in the transition zone - bears more similarity to the seawardmost distribution (which relates to the mean flow under an unbroken wave) than to the shoreward breaking wave undertow distributions. This apparent lag between wave breaking and the generation of undertow has been noted on several occassions in the literature (i.e. Nadoaka and Kondoh, 1982 and Longuet-Higgins, 1983 among others). Within the transition zone, the forcing of the undertow due to the reduction in radiation stress is not yet realised; this demonstrates the importance of considering the influence of the transition zone shift on the prediction of mean return flow.

The predictions of undertow under random waves for two laboratory tests with and without the use of a revised Q_b are shown in Figures 8 and 9 (the data for these two tests were given by Roelvink and Stive, 1989 and Sato et al, 1988 respectively). In both cases, the influence of the transition zone has a considerable effect on the predictions; the results with a revised Q_b provide a much better match to the measured data. Field measurements of the cross-shore distributions of undertow (along with the important recordings of profile shape and inshore wave climate) are generally unavailable, however, as a demonstration of a field case, the predicted undertow for the DUCK85 Case 5 example (corresponding to Figure 3) is compared to the measurements from two electromagnetic current meters in Figure 10. It is difficult to assess the validity of the predictions from this data, however, the exercise does reveal the importance of accounting for the the transition zone shift in the predictions.

It has become abundantly clear that the distribution of undertow across the profile is a primary factor in the reshaping of beach profiles during erosion events (see Nairn, 1990a and Roelvink and Stive, 1989). A brief example of the influence of the transition zone shift on profile development is shown in Figure 11. This laboratory test corresponds to the undertow prediction given in Figure 8, the test duration was 12 hours. Again, the importance of considering the transition zone effect is revealed by a comparison of the predictions with and without the shift to the measured profile change. Specifically, the bar position is shifted too far seaward in the numerical model test without the transition zone influence (i.e. using the unrevised value for the fraction of broken waves, Q_b.)

A field experiment to measure alongshore sand transport in the surfzone was conducted at the Field Research Facility of the Coastal Engineering Research Centre, U.S. Army Corps of Engineers at Duck, North Carolina (see Kraus et al, 1989). Eight tests were performed in September of 1985 as part of the DUCK85 programme using a series portable sand traps deployed across the surfzone (the traps consisted of polyester sieve cloth streamers suspended on a rack). Two electromagnetic current meters were also deployed to monitor the cross-shore and longshore flow velocities in the surfzone. For a selected test, the cross-shore flows were presented in Figure 10 and the wave transformation prediction including the revised fraction of broken waves accounting for the transition zone influence were given in Figure 3. A demonstration of the effect of using the revised fraction of broken waves in the prediction of longshore currents for the same DUCK85 test is shown in Figure 12. The peak longshore current is reduced and predicted velocities in the outer part of the surfzone have been considerably diminished. The influence is large due to the low steepness of the incident wave (H_{rms} = 0.31 m, T = 9.7 s), indicating that a plunging breaker and a correspondingly large transition zone width would have existed. The predicted velocities compare well with the field measurements, however, the two isolated recordings are not sufficient to verify the transition zone phenomenon.

In the numerical model used for these investigations, both the longshore and cross-shore sediment transport rates are calculated using a modified version of the Energetics approach adapted for coastal sediment transport by Bowen (1980) and Ballard (1981) from the original formulation of Bagnold (1963) for sediment transport in rivers. Modifications to the cross-shore and alongshore components of this approach are given in Nairn (1990a) and Nairn (1990b) respectively. Simply stated, the Energetics approach is based on the concept that the wave action acts to support the sediment in bed and suspended load which is then advected by mean currents, orbital velocity asymmetry and gravity. Therefore, the distribution of the longshore current across the profile is a critically important element of the alongshore transport estimate. This is reflected in a comparison of the predicted (with and without the transition zone influence) and measured alongshore transport rates given for the selected test of the DUCK85 field experiment in Figure 13. Clearly, this figure serves indirectly to confirm the extent of the transition zone influence on the generation of longshore currents.

DISCUSSION

The existence of a transition zone where wave decay and turbulent energy production occur unaccompanied by energy dissipation is clearly evident for monochromatic waves. The processes which are associated with the reduction in radiation stress (caused by the dissipation of wave energy) - including wave setup, undertow and longshore current - are initiated at the inner limit of the transition zone instead of at the breakpoint due to the lag between the production and the dissipation of wave energy from wave decay after breaking. The transparency of the problem in monochromatic wave situations allows for an empirical expression to be developed relating the dimensionless transition zone width (i.e. the depth at the inner limit of the transition zone divided by the depth at breaking) to the surf similarity parameter evaluated entirely with breakpoint parameters (see Equation 2). The dimensionless width is found to be greater for plunging breakers than for spilling breakers.

The clarity of this phenomenon is obscured for random waves since the width of the surfzone and the transition zone varies with each individual wave in the incident climate. However, if wave-wave interaction is ignored in the surfzone, it may be assumed that each individual wave behaves as a wave from a monochromatic wave train and the expression derived for transition zone width should be equally applicable to this situation. Neglecting wave-wave interaction is probably an acceptable assumption since the larger waves will have a celerity proportional to the depth based on the shallow water assumption and thus the possibility of one wave overtaking another is limited. Therefore, whilst the influence of the transition zone shift is less transparent in random wave surfzones, it is nonetheless very important to consider in the numerical prediction of the time-averaged values of wave setup, undertow and longshore current. With the aid of field and laboratory experiments it has been demonstrated that transition zone influence has a significant effect on the generation of time-averaged currents and the associated sediment transport (i.e. both alongshore and cross-shore).

Two techniques are presented for the description of the transition zone influence on random wave processes. The empirical approach has the benefit of responding to different incident wave conditions. However, the development of the analytical technique will ultimately allow for a better understanding of the physical phenomena.

Caution is advised in applying Equation 2 to situations of waves with very low steepness breaking on steep slopes - especially for surging and collapsing breakers (i.e. high values of the surf similarity parameter at breaking) - as there are indications that the transition zone width is over-estimated for these cases. More data on the monochromatic transition zone width is required to improve the reliablity of Equation 2 in these instances. There is also a need to verify directly the transition zone influence in random waves through the analysis of a time series of simultaneous measurements of velocity, turbulence and water surface elevation.

REFERENCES

Bagnold, R.A. (1963). Beach and Nearshore Processes. In The Sea. Vol. 3. ed., M.N. Hill. Interscience, N.Y.

Bailard, J.A. (1981). An Energetics Total Load Transport Model for a Plane Sloping Beach. J.of Geophys. Res. Vol. 86, No. C11. pp. 10938-10954.

Basco, D.R. and Yamashita, T. (1986). Toward a Simple Model of the Wave Breaking Transition Region in Surfzones. Proc. of the 20th Conf. on Coastal Eng., ASCE. pp. 955-970.

Basco, D.R. (1985). A Qualitative Description of Wave Breaking. J. of Waterway, Port, Coastal and Ocean Eng., ASCE. Vol. 111, No. 2. pp. 171-188.

Battjes, J.A. and Janssen, J.P. (1978). Energy Loss and Setup Due to Breaking of Random Waves. Proc. of the 16th Conf. on Coastal Eng., ASCE. pp. 569-588.

Bowen, A.J. (1980). Simple Models of Nearshore Sedimentation: Beach Profiles and Longshore Bars. In The Coastline of Canada. ed., S.B. McCann. pp. 1-11.

Deigaard R. and Fredsoe J. (1989). Shear Stress Distributions in Dissipative Water Waves. Coastal Engineering. Vol. 13. pp. 357-378.

DeVriend, H.J. and Stive, M.J.F. (1987). Quasi-3D Modelling of Nearshore Currents. Coastal Engineering. Vol. 11. pp. 565-601.

Kraus, N.C., Gingerich, K.J. and Dean Rosati, J. (1989). DUCK85 Surf Zone Sand Transport Experiment. CERC Rept. No. 89-5. 48 pp.

Longuet-Higgins, M.S. (1983). Wave Setup, Percolation and Undertow in the Surfzone. Proc. of the Royal Society of London. A390. pp. 283-291.

Nadoaka, K. and Kondoh, T. (1982). Laboratory Measurements of Velocity Field Structure in the Surf Zone by LDV. Coastal Eng. in Japan. Vol. 25. pp. 125-145.

Nairn, R.B. (1990a). Prediction of Cross-Shore Sediment Transport and Beach Profile Evolution. Ph.D. Thesis. Imperial College, University of London. 391 pp.

Nairn, R.B. (1990b). Validation of a Detailed Alongshore Transport Model. Proc. Euromech 262, Sand Transport in Rivers, Estuaries and the Sea. Wallingford.

Okayasu, A., Watanabe, A. and Isobe, M. (1990). Modeling of Energy Transfer and Undertow in the Surf Zone. Proc. of the 22nd Conf. on Coastal Eng., ASCE.

Roelvink, J.A. and Stive, M.J.F. (1989). Bar Generating Cross-Shore Flow Mechanisms on a Beach. J. of Geophys. Res. Vol. 94, No. C4. pp. 4785-4800.

Sato, S., Fukuhama, M. and Horikawa, K. (1988). Measurements of Near-Bottom Velocities in Random Waves on a Constant Slope. Coastal Eng. in Japan. Vol. 31, No. 2. pp. 219-229.

Southgate, H.N. (1989). A Nearshore Profile Model of Wave and Tidal Current Interaction. Coastal Eng., Vol. 13. pp. 219-245.

Svendsen, I.A. (1984). Wave Heights and Setup in a Surfzone. Coastal Eng., Vol. 8. pp. 303-329.

Svendsen, I.A., Madsen, P.A. and Hansen J.B. (1978). Wave Characteristics in the Surfzone. Proc. of the 16th Conf. on Coastal Eng., ASCE. pp. 520-539.

Swart, D.H. (1978). Vocoidal Water Wave Theory, Volume 1: Derivation. National Research Institute for Oceanology, South Africa. CSIR Rept. No. 357. 137 pp.

Visser, P.J. (1984). Uniform Longshore Current Measurements and Calculations. Proc. of the 19th Conf. on Coastal Eng., ASCE. pp. 2192-2207.

Fig.1 - Regular Wave Height and Setup
Hansen and Svendsen (1979) Case N

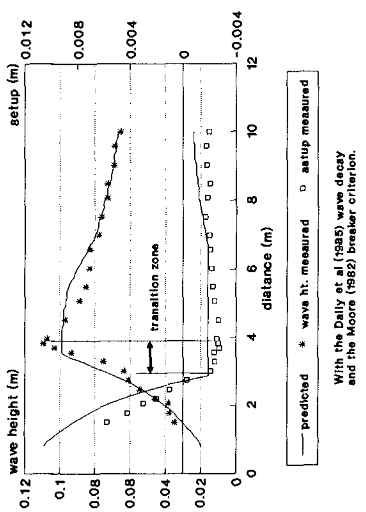

Figure 2 - Transition Zone Width
Empirical Approach

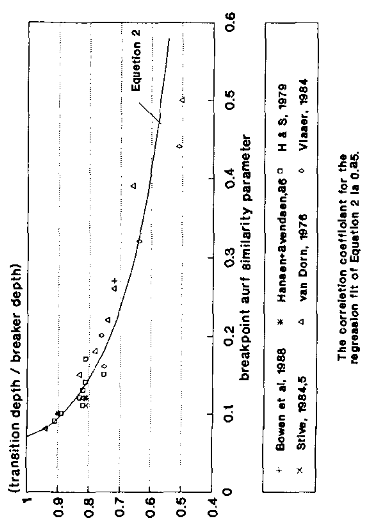

Figure 3 - Wave Transformation
DUCK85 Case 5 - Hrms = 0.31 m, T = 9.7 s

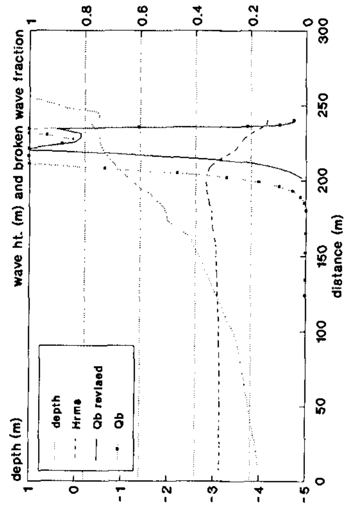

Fig. 4 - Random Wave Height and Setup
Battjes and Janssen (1978) Test HJ2

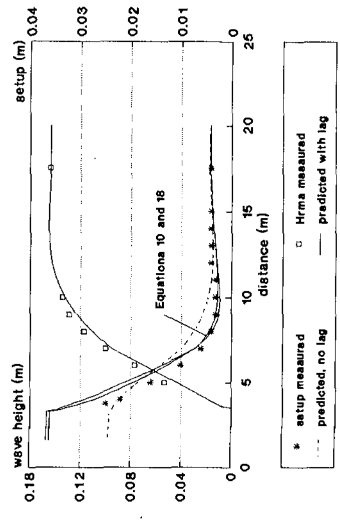

Fig. 5 - Random Wave Height and Setup
Battjes and Janssen (1978) Test HJ12

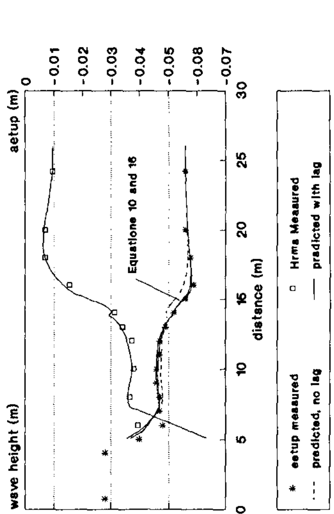

Figure 6a - Transition Zone Width
Analytical Approach
vs. Deepwater Surf Similarity Parameter

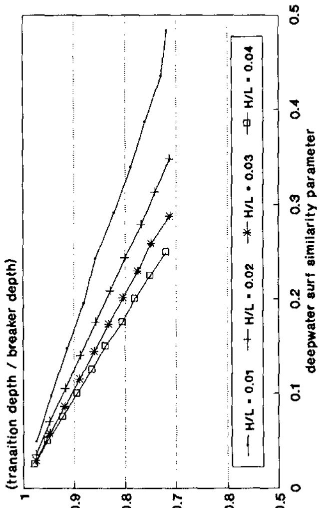

Figure 6b - Transition Zone Width
Analytical Approach
vs. Breakpoint Surf Similarity Parameter

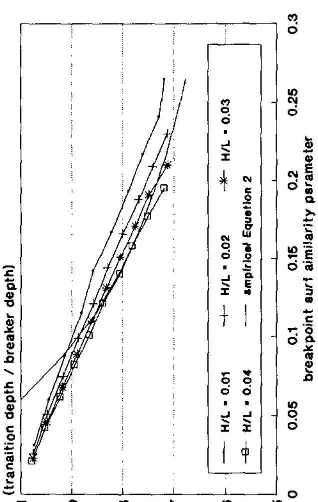

Figure 6c - Transition Zone Width
Analytical Approach vs. Beach Slope

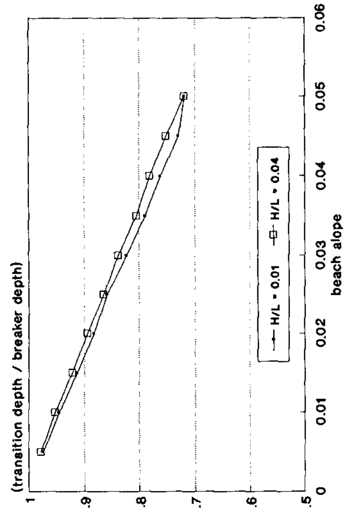

Figure 7 - Regular Wave Undertow
Nadoaka and Kondoh (1982) data

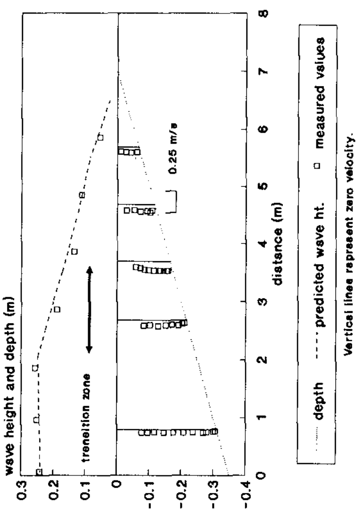

Figure 8 - Random Wave Undertow
Delft Case 1 - H = 0.123 m, T = 2 s

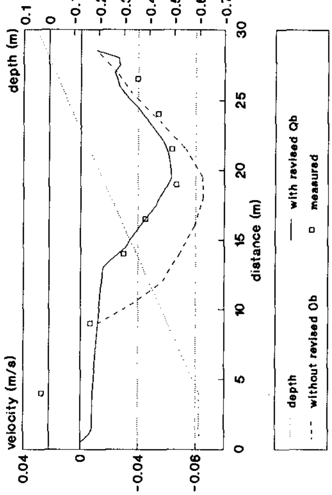

Figure 9 - Random Wave Undertow
Sato Case 3 - Hrms = 0.036 m, T = 0.92 s

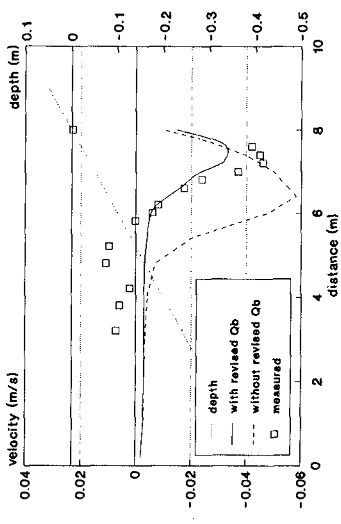

Figure 10 - Random Wave Undertow
DUCK85 Case 5 - H = 0.31 m, T = 9.7 s

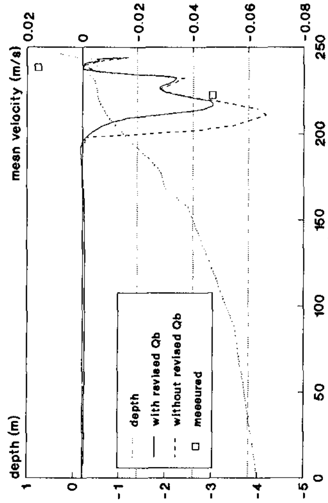

Figure 11 - Profile Change
Delft Case 1 after 12 hrs.

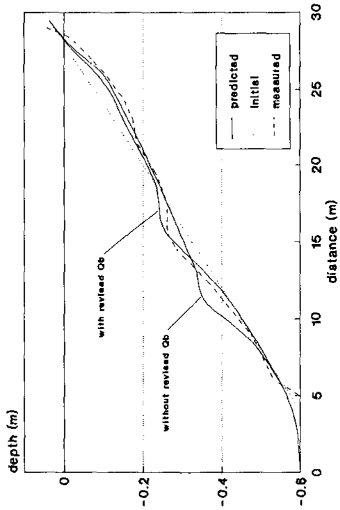

Figure 12 - Longshore Current
DUCK85 Case 5 - H = 0.31 m, T = 9.7 s

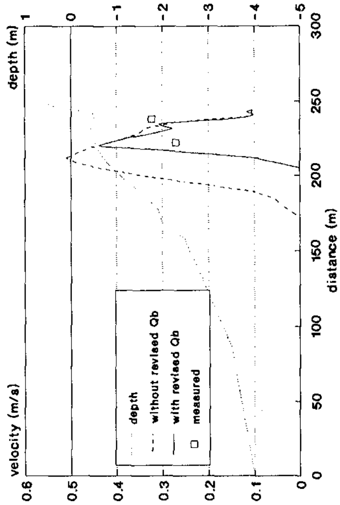

Figure 13 - Alongshore Transport
DUCK85 Case 5 - Energetics Approach